Lecture 20
Auger Electron Spectroscopy

Auger – history cloud chamber

Although Auger emission is intense, it was not used until 1950's.

Evolution of vacuum technology and the application of Auger Spectroscopy - Advances in space technology

Various ways to estimate Auger electron kinetic energy

$$E_{KL1\,L23} = E_k^{(z)} - E_{L1}^{(z)} - E_{L23}\,(z + \Delta) - \phi_A$$
$$= E_k^{(z)} - E_{L1}^{(z)} - E_{L23}^{(z)} - \Delta[E_{L2,3}\,(z+1) - E_{L2,3}^{(z)}]$$

$$E_{xyz} = E_x - \tfrac{1}{2}\,(E_x(z) + E_y(z+1)) - \tfrac{1}{2}\,(E_2(z) + E_2(z+1)) - \phi_A$$

Δ has been found to vary from 0.5 + 1.5.

Relaxation more important than ESCA.

Auger energy is independent of sample work function. Electron loses energy equal to the work function of the sample during emission but gains or loses energy equal to the difference in the work function of the sample and the analyser. Thus the energy is dependent only on the work function of the analyser.

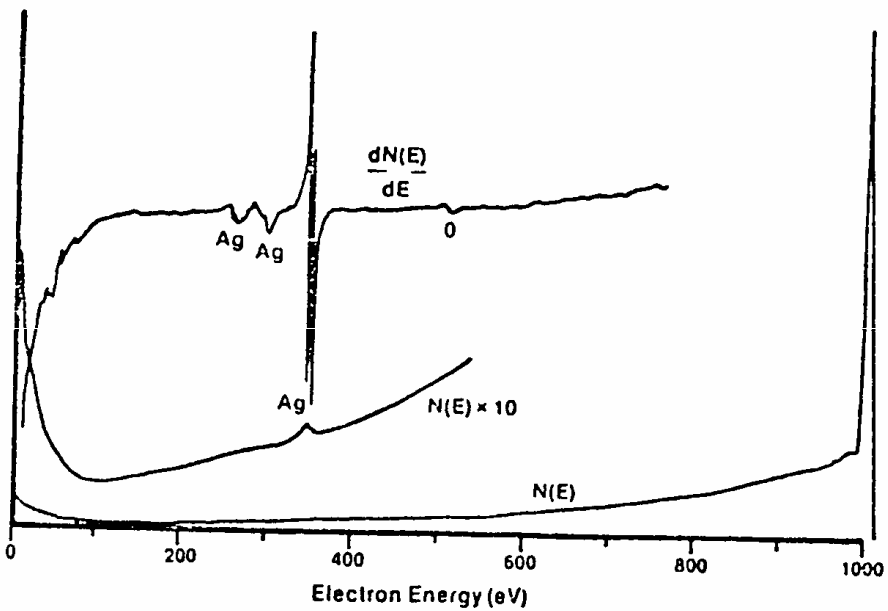

Fig. 1. Energy distribution and derivative of the energy distribution of secondary electrons from a silver target with an incident beam of 1000 eV electrons.

Use of dN(E)/dE plot

Instrumentation

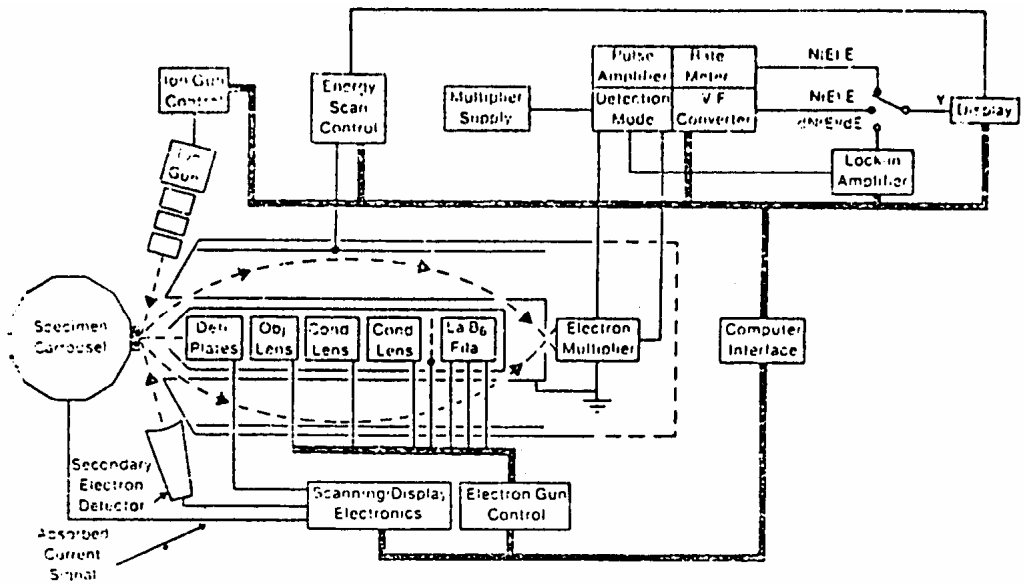

Fig. 4. Schematic layout of electron optics and electronics for a scanning Auger spectrometer.

Early analysers

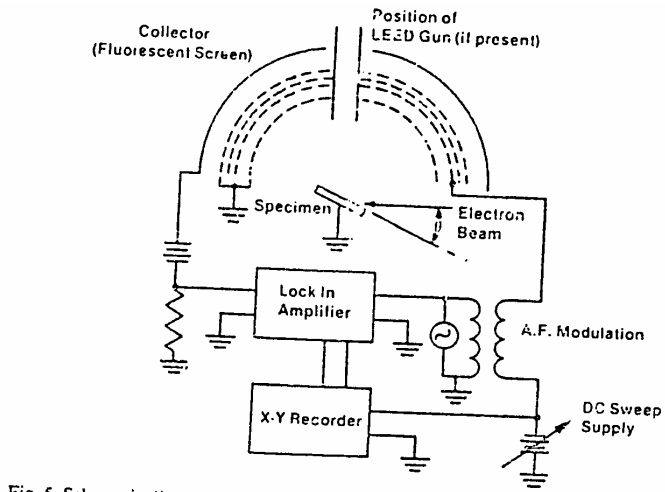

Fig. 5. Schematic diagram of a retarding field analyzer.

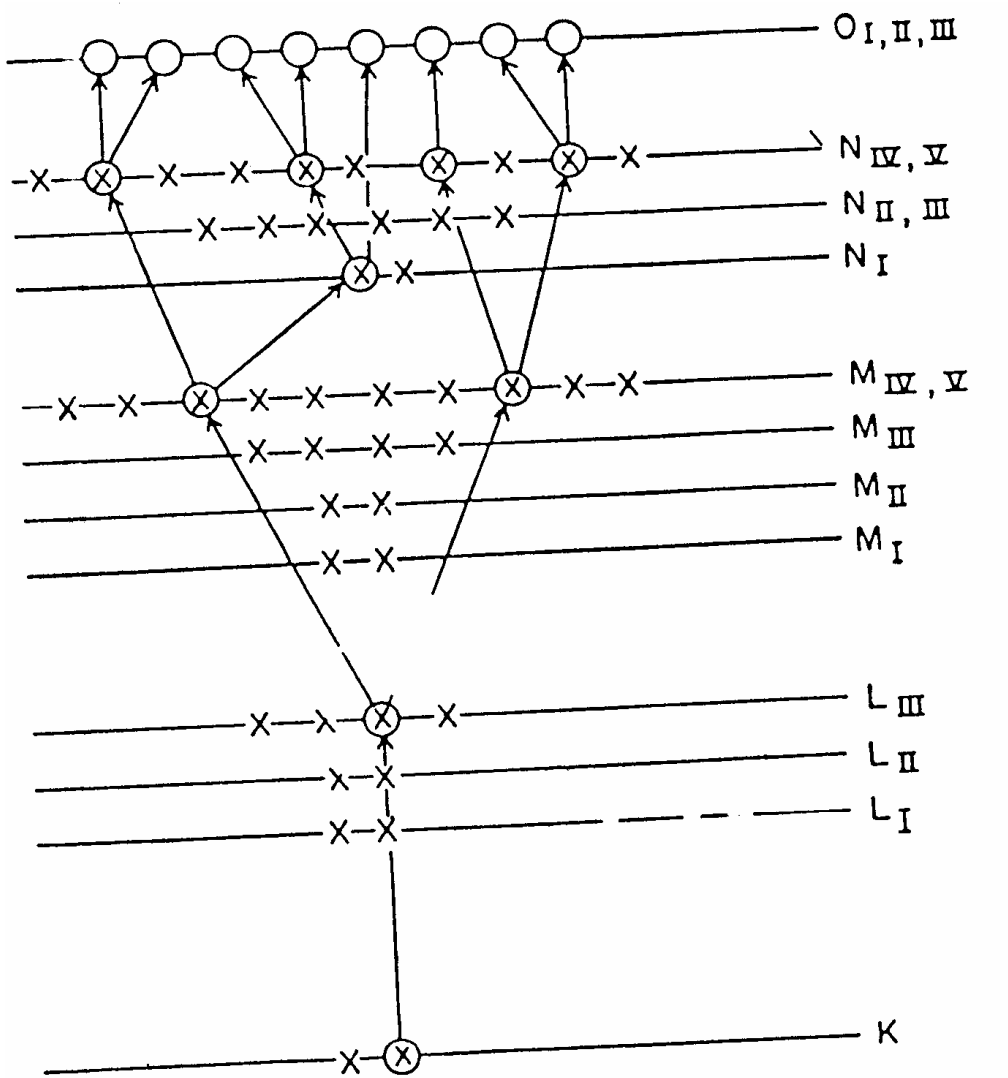

FIGURE 6.2. Schematic representation of a vacancy cascade in Xe. ×, Electrons; ○, vacancies; ⊗, vacancies that were subsequently filled by electrons.

What happens to the system after Auger emission

Chemical differences

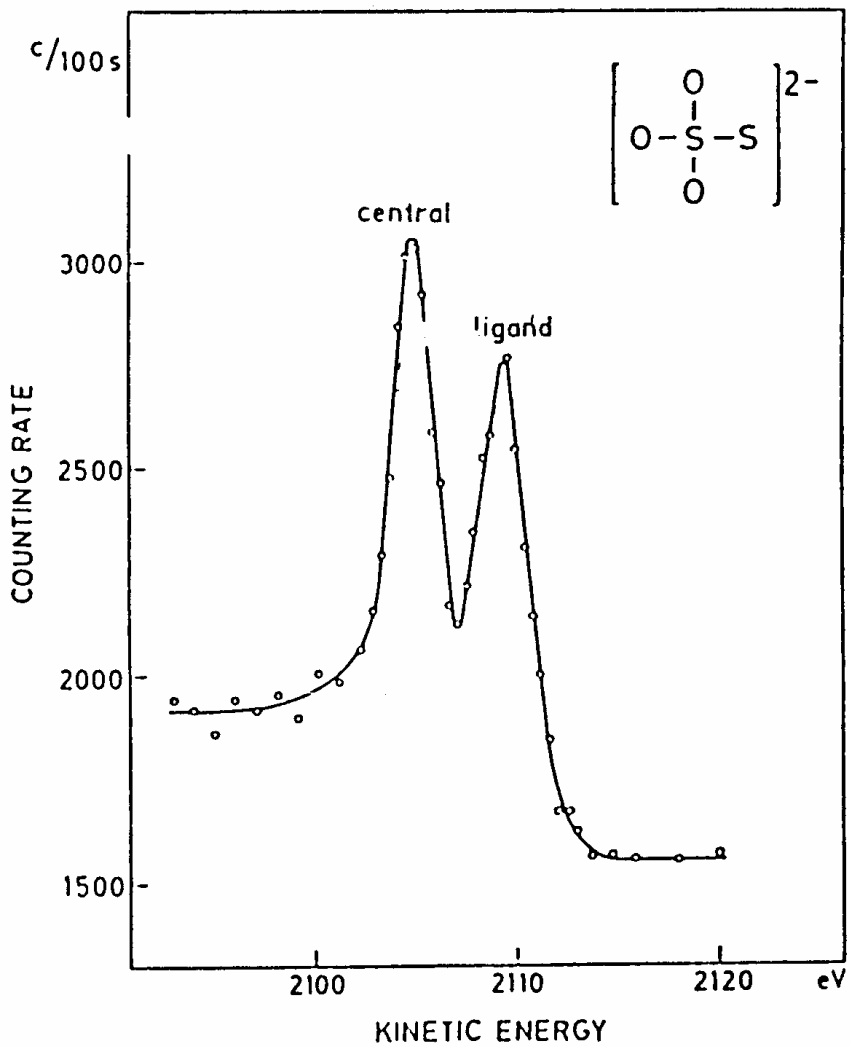

FIGURE 6.6. The *K–LL* [$2s^2 2p^4$ ($^1D_2$)] Auger spectrum of sulfur for $Na_2S_2O_3$, showing two peaks corresponding to differences in chemical environment. [Reproduced from Fahlman *et al.*[32]]

When core electrons are involved in Auger, the chemical shifts are similar to XPS.

For $S_2O_3^-$, the chemical shifts between +6 and –2 oxidation states are 7eV for k shell and 6 eV for α_p. The chemical shift for Auger is given as $\Delta E = \Delta E_1 - 2\Delta E\ (L_{II,III}) = 5$ eV

The experimental value is 4.7 eV

Chemical sifts of core levels - change in relaxation energy.

Characteristics

Electron and photon excitation (XAES). Auger emission is possible for elements z >3. Lithium is a special case.
No Auger in the gas phase but shows in the solid state.

Auger emission from outer shells is constant with z. Thus KLL, LMM, MNN series etc can be used for elemental analysis.
Detection limits are 0.1 % atomic.

Spatial resolution ~ 50nm.

Depth resolution is better normal to the surface than in the plane.
Mean free path.

Complications

Plasmons, doubly ionized initial electron states, multiplet splitting, Multiple excitations, Coster-Kronig transitions. Super coster-Kronig transitions.

Volume and surface plasmons. Inter and intra band transitions or shake up

Coster – Kronig L_1L_3 X X $\neq$ L
Super Coster Kronig L_1L_3 X X = L
Cross over transitions. Eg. MgO. Hole in O may be filled by electron from Mg - Non isotropic Auger emission from single crystals. Diffraction.
Isotropic from polycrystalline samples.

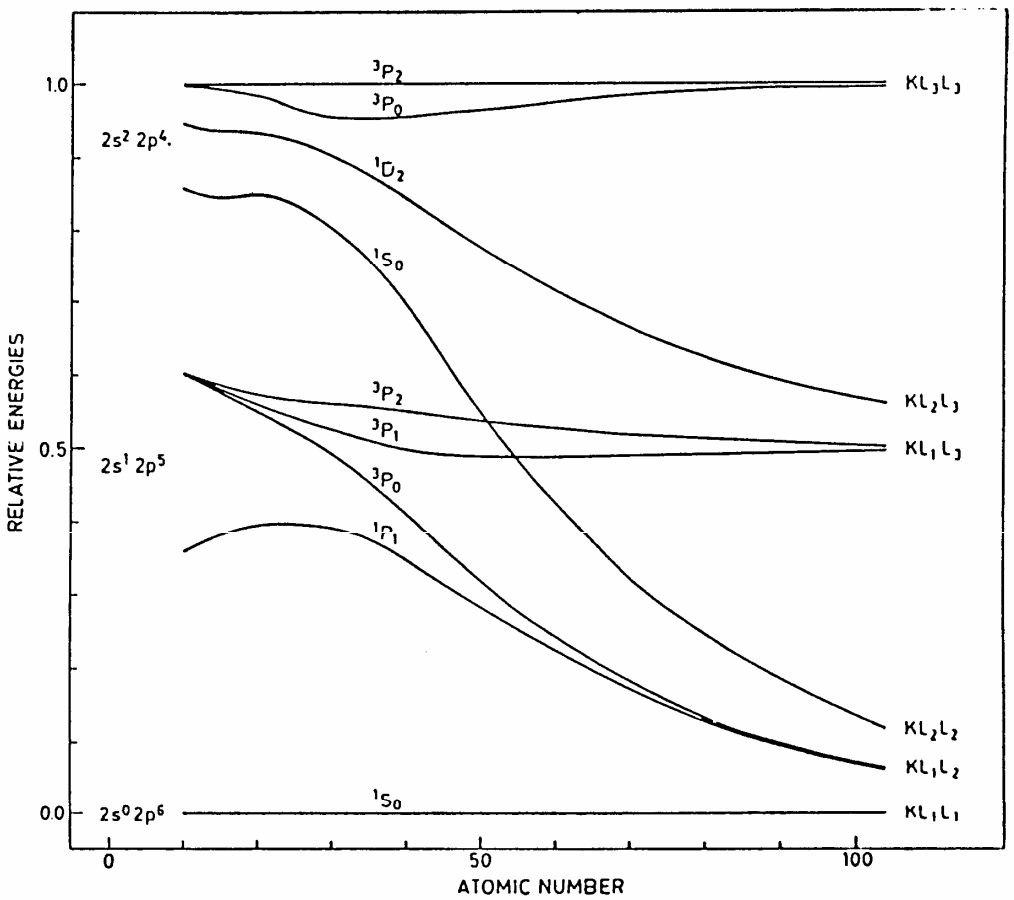

FIGURE 6.1. Relative line positions in *K–LL* Auger transitions as a function of *Z*. At low *Z* one has nearly pure *L–S* coupling and six lines. However, the $2s^2 2p^4\ ^3P$ is strongly forbidden in the nonrelativistic region. At high *Z* one has nearly pure *jj* coupling and six lines; nine lines are possible in the intermediate coupling region. [Reproduced from Siegbahn *et al.*,[13] Figure 4.1.]

Chemical effects

Relaxation is larger than in XPS. Chemical effects in XPS will not directly correspond with those of Auger. The difference between XPS and Auger energies is called Auger parameter, used to characterise the chemical state. More changes for transitions involving valence states.

Applications in:

Corrosion
Adhesion
Catalysis
Chemical characterization
Surface reaction
Electronic materials

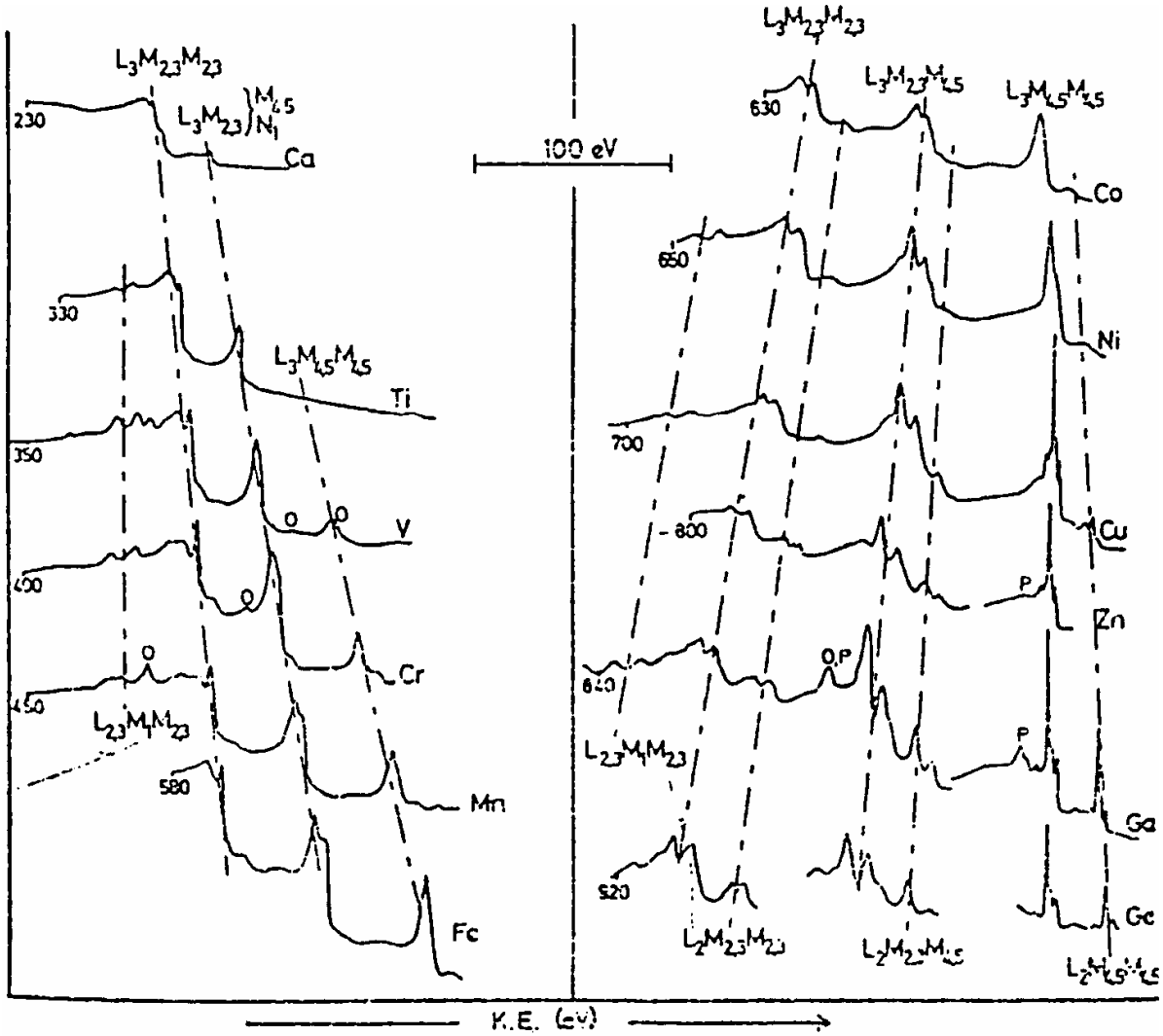

Fig. 18. LMM Auger spectra of elements Ca to Ge. Spectra of samples with low contamination levels have been chosen but some of the peak labelled O may contain contributions from oxygen XPS and Auger peaks. Peaks labelled P are due to plasmon-like energy losses. All spectra, except that of Ge, were recorded with instruments retarding the electrons to a constant analyser pass energy (increased sensitivity at low K.E.) Sources of spectra: Co, Ti, Cr, Mn, Co, Cu (ref. 82); V (refs 82, 189, 218); Fe (ref. 189); Ni (refs 82, 218); Zn (refs 55, 123, 219, 220); Ga, Ge (refs 82, 55)

High resolution AES using photons

Beam effects
Electron stimulated desorption
Core hole lifetimes are smaller than vibrational time scale and dissociation is not important. But the core hole will lead to electron cascade and multiply charged ion many result which will have a large dissociation probability.

Photon induced desorption is also important but photon fluxes are much lower. Beam effect are important.

Excitation cross sections in XAES and EAES are different.

Threshold effects in Auger

Decay of the core hole leading to double ionization post collision effects changing peak energies.

$L_{2,3}$ spectra of Mg with Mg K_α and Al K_α.

Double ionization satellite in Al K_α not in Mg K_α.

By electrons it is found that the threshold for double ionization is ~120 eV, but the satellite was not sharp as with X-ray excitation.

When KE of outgoing electron is low, Auger emission can happen in the field of receding electron. Energy available can be re-partitioned. If threshold electron is used, Auger emission happens in the field of The receding electron. These interaction are called post collision interactions.

Plasmon gains and losses

Plasmon gain occurs by intrinsic mechanism. For it to occur, plasmon excited should be at the site of ionization, therefore it cannot be extrinsic.

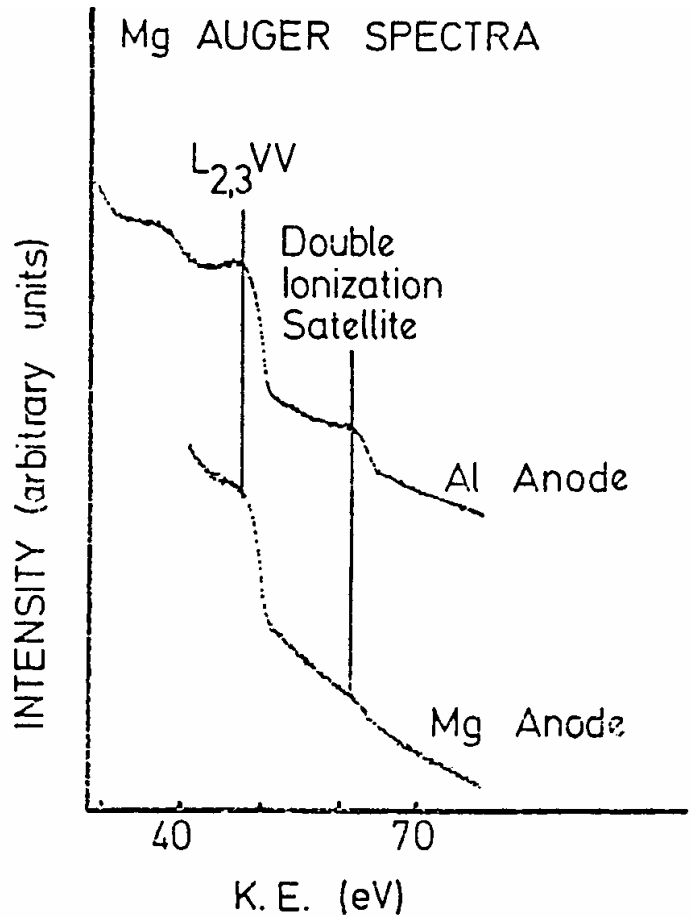

Fig. 13. Increase of the Mg LVV double ionization satellite intensity in XAES as the exciting X ray energy is increased above the Mg K ionization threshold.[175]

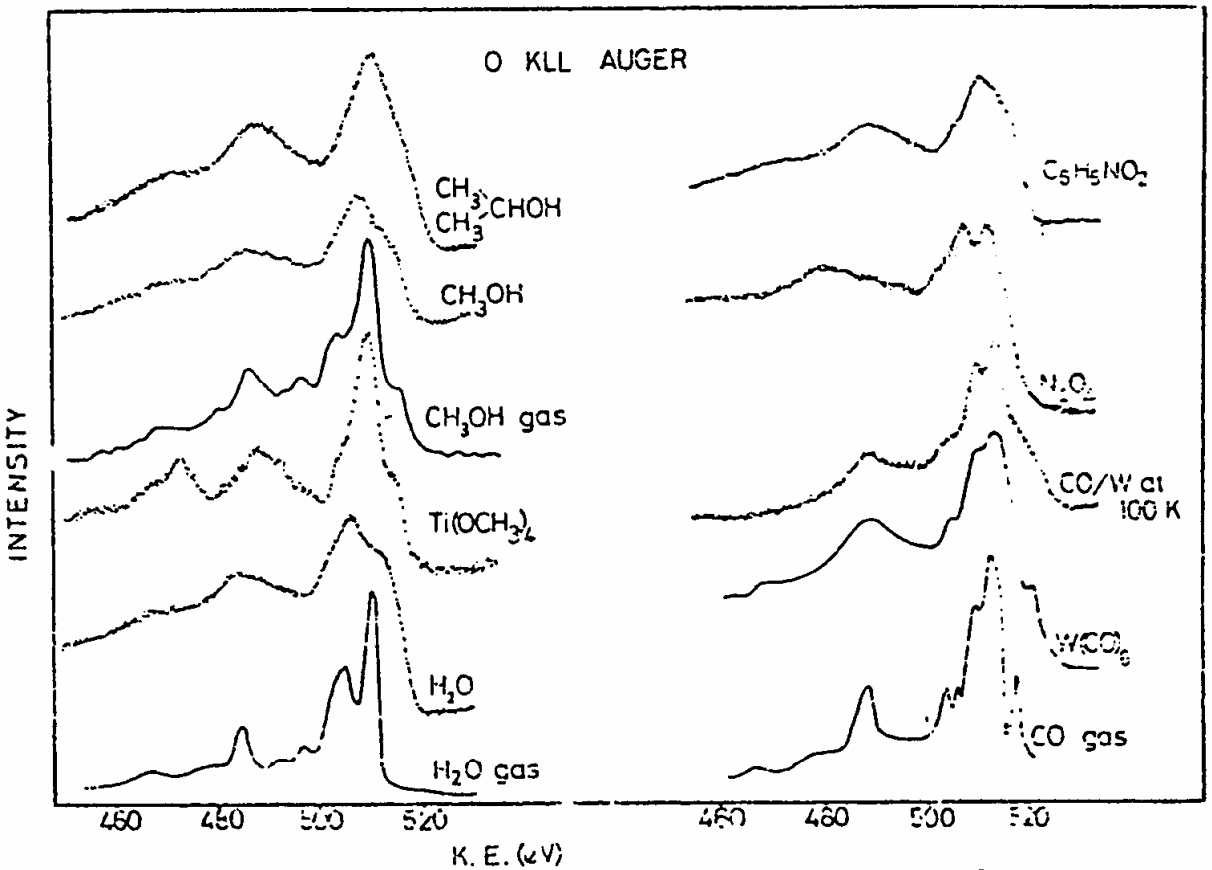

Fig. 26. O KLL Auger spectra from oxygen in a variety of chemical environments. All ... are from condensed layers unless otherwise stated. The spectra of H_2O gas, CH_3OH ... and CO gas have been shifted by respectively approximately 12, 11, and 16 eV to higher K.E. to allow for the different reference levels and relaxation effects (Section III.F) and to line up the characteristic features as well as possible. Differences in the low K.E. background are not significant as different instruments have been used to record the spectra. References: H_2O gas (79, 253, 256), H_2O, $Ti(OCH_3)_4$, CH_3OH, $(CH_3)_2CHOH$, $W(CO)_6$, N_2O_2, and $C_5H_5NO_2$ (274); CH_3OH ... (241, 242); CO gas (241, 255).

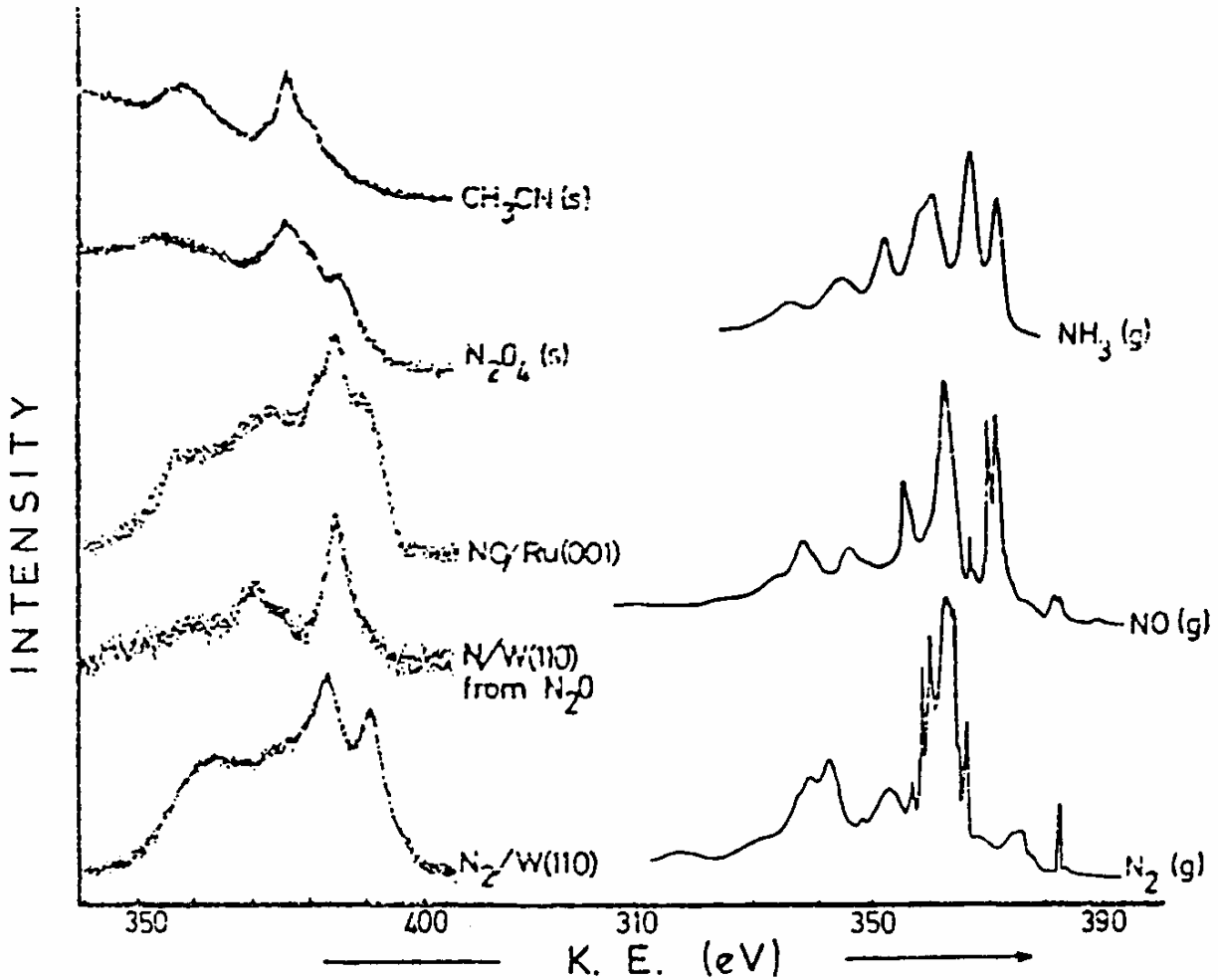

Fig. 27. N KLL Auger spectra from nitrogen in a variety of chemical environments. References NH_3 gas (259); NO and N_2 gas (258); CH_3CN and N_2O_4 (234); NO Ru(001) (252); N/W(110) (249) N_2/W(110) (249, 260).

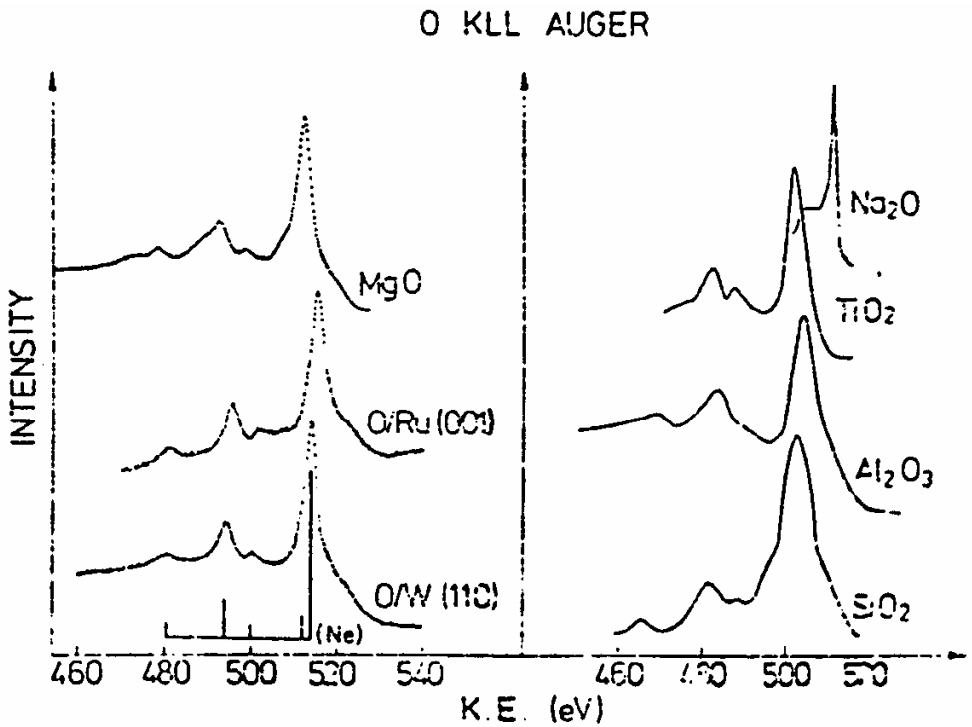

Fig. 23. Oxygen KLL Auger spectra from MgO,[231,232] oxygen chemisorbed on Ru(001)[234,245] and W(110),[248] Na_2O,[84] TiO_2,[97] Al_2O_3,[82] and SiO_2.[235] The *relative* spacings and intensities of Ne KLL lines[170] are also shown.

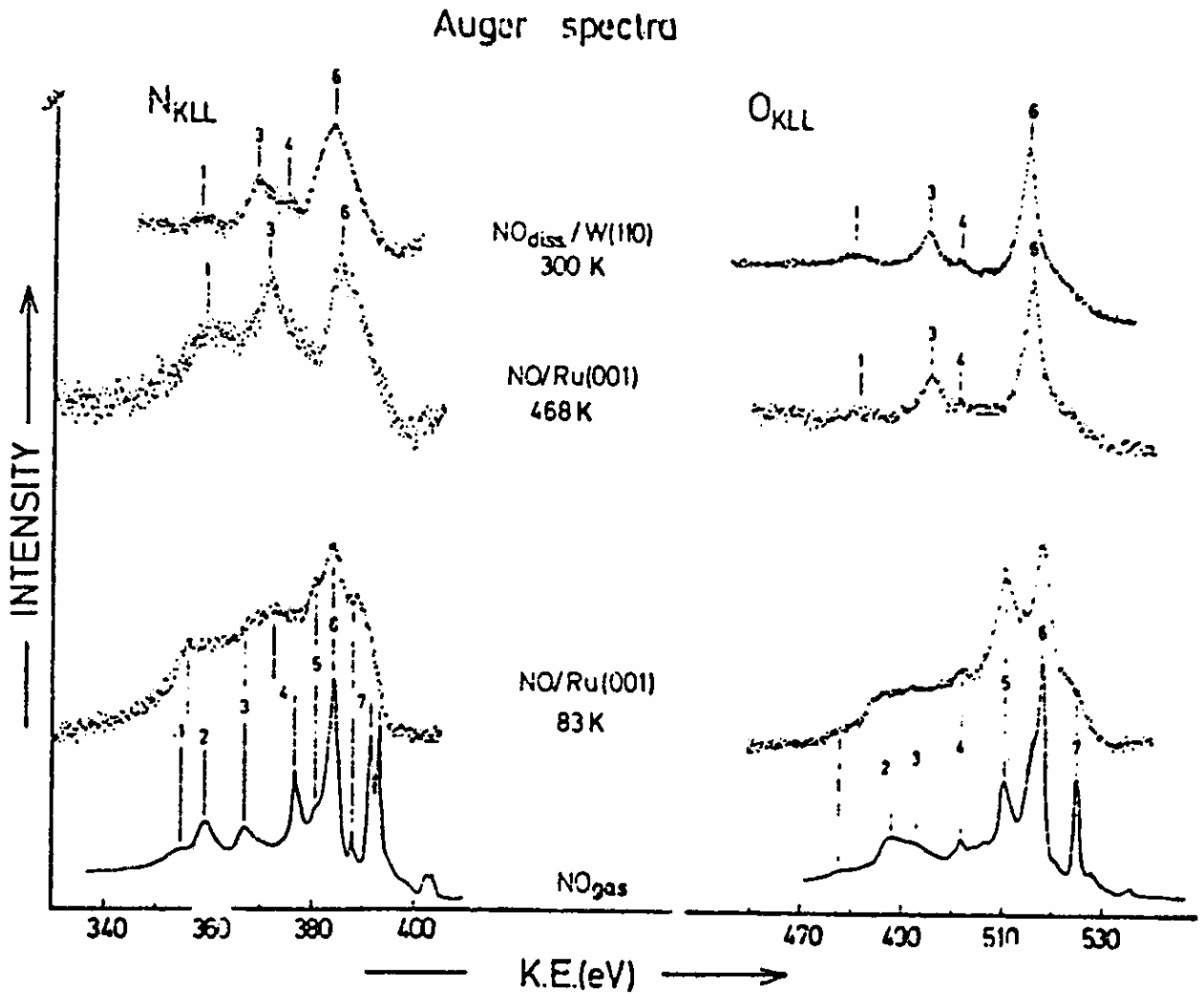

Fig. 22. Comparison of O KLL and N KLL Auger spectra from NO gas[250] and NO adsorbed on Ru(0001) at low temperatures and then warmed to 468 K. On warming the NO is seen to dissociate as shown by the similarity of O KLL spectra to those of chemisorbed oxygen shown in Fig. 23. The dissociated NO spectra are similar to those of NO on W(110) where dissociative adsorption is found at both 100 K and 300 K.[249] (From ref. 252).

Auger microscopy